Research Article | Vol. 27, No. 12 | 10 Jun 2019 | OPTICS EXPRESS 16571
Optics EXPRESS

Spectrally tunable chiral Bragg reflectors for on-demand beam generation

B. A. KOWALSKI,[1] V. P. TONDIGLIA,[2] K. M. LEE,[2] D. R. EVANS,[2] T. J. WHITE,[2] AND M. S. MILLS[2,*]

[1] *University of Colorado, Boulder, CO, USA*
[2] *Air Force Research Laboratory, Wright-Patterson Air Force Base, OH, USA*
[*] *matthew.mills.25@us.af.mil*

Abstract: We demonstrate the generation of spectrally tunable phase-dependent wavefronts, using the 2D Airy as the primary test case, via a polymer-stabilized cholesteric liquid crystal (PSCLC) element. Specifically, we use a novel spatial light modulator (SLM) based projection system to photo-align the initial helix angle landscape of the PSCLC so that it imparts the appropriate cubic phase profile to the reflected beam. This element is spectrally selective, with a reflection bandwidth of $\approx$ 100 nm, and electrically tunable from λ = 530 nm to 760 nm. Under both green and red laser illumination, the element is shown to conditionally form an Airy beam depending on the position of the electrically tailored reflection band. We briefly demonstrate the generality of this approach by producing PSCLC elements which form a computer-generated hologram and a higher-order Mathieu beam.

1. Introduction

Cholesteric liquid crystals (CLCs) form chiral Bragg reflectors via self-assembly. Recently it has been shown that variations in the initial helix angle of the CLC impart a geometric or Pancharatnam-Berry phase modulation on the reflected beam (illustrated in Fig.1) [1, 2]. Appropriate spatial patterning, both in context of CLCs and other similar systems, of the helix angle landscape has been used to impart phase profiles that correspond to various spin-orbit related functionalities, including beam focusing, beam steering, polychromatic manipulations, and generation of vortex beams and other exotic beam modes [3–16]. We propose here that this approach is also compatible with the wide range of previously demonstrated techniques for dynamic tuning, broadening, and switching of reflection bands, particularly in polymer-stabilized cholesteric liquid crystal systems.

To demonstrate the utility of this approach, we turn to the problem of generating 2D Airy beams, since these exhibit distinctive properties, and require relatively delicate control over a phase-front. Briefly, Airy beams are non-diffracting beam modes which freely-accelerate during propagation [17, 18]. Since the initial prediction [17] and observation of the Airy beam [19], entire families of accelerating wavefronts have been conceived [20] in both the paraxial and non-paraxial regimes including, for example, the parabolic [21], Mathieu [22], Half-Bessel [23], and Weber beams [24]. In recent years, their unique self-bending and self-healing properties have been exploited in a broad range of applications including microscopy, optical trapping, imaging through turbulent media, abruptly focusing beams, and curved plasma filaments in air [12–16, 25–31].

However, large-scale utilization of these exotic beams is hindered by expensive fabrication techniques needed to prepare the necessary optical components. The 2D Airy beam, for instance, requires a cubic phase variation with respect to transverse position; typically this is imparted by either a spatial light modulator [19] – which can be expensive, bulky, and offers limited efficiency – or a transparent phase mask fabricated via focused ion beam lithography – which is a costly static element designed only for a particular wavelength. These considerations have motivated the

#360073 https://doi.org/10.1364/OE.27.016571
Journal © 2019 Received 22 Mar 2019; revised 14 May 2019; accepted 14 May 2019; published 29 May 2019

Optics EXPRESS

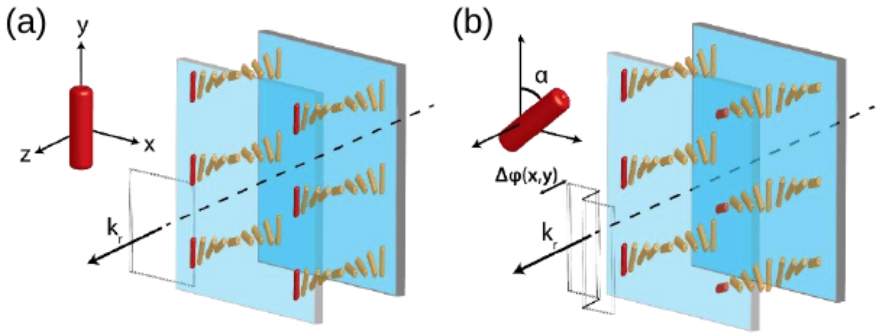

Fig. 1. (a) Cholesteric liquid crystals in a uniform alignment cell self-assemble into a chiral Bragg reflector. An incident beam with the matching circular polarization is reflected with a flat phase front. (b) In the case of non-uniform alignment, regions with an initial helix angle of α impart a Pancharatnam-Berry or geometric phase modulation of 2α upon the reflected beam.

development of compact, dynamically switchable phase masks [32]. For example, transmissive cubic-phase elements have been realized in photo-aligned holographic polymer-dispersed liquid crystals [33] and polymer-stabilized blue-phase liquid crystals via lithographically patterned electrodes [34].

In this letter, we instead engineer a reflective optical element which exploits helix angle patterning of a PSCLC. This element selectively imparts an arbitrary geometric phase to light within the reflection band, while light outside the reflection band is transmitted with no phase modulation. Crucially, we show that the reflection band of this device can then be shifted via externally applied voltage – allowing one to dynamically tune which wavelength will efficiently diffract the prescribed phase profile. We emphasize that this scheme enables independent design of the reflection band (via the pitch of the PSCLC), and the beam shape (via the helix angle landscape). Furthermore, the element is achromatic in the sense that the same geometric (Pancharatnam-Berry) phase is imparted to all wavelengths as they fall within the tunable reflection band.

2. Producing a PSCLC element with an imposed geometric phase

The initial helix angle landscape is templated by a patterned alignment surface. Following [3, 4], this alignment surface comprises a thin layer of dye molecules containing azobenzene moieties, that can be reoriented by exposure to relatively low doses of linearly polarized light. Thus, an arbitrary desired pattern of helix angles can be recorded by exposure to light of pixelwise varying linear polarization angles.

We use a Meadowlark SLM for the experiment motivated both by the desire for arbitrary and reconfigurable patterning and a high pixel count in order to maximize the element's eventual diffraction efficiency (920 x 1152 pixels spaced at 16 μm). However, it is a relatively uncommon goal to convert the phase modulation from a conventional reflective SLM (LCoS-SLM) into a modulation of linear polarization angle. Here we propose a novel optical layout which accomplishes this using only a single reflection from the SLM (Fig. 2). This is distinct from more complex previously reported layouts in which an incident beam is reflected twice in succession from two different regions of the SLM [35]. Here, instead, the patterned pixel count is equal to the full pixel count of the SLM. Finally, the polarization pattern is imaged onto the alignment cell, via an imaging relay which enables Fourier plane filtering, as well as demagnification to improve the effective numerical aperture of the produced diffractive element.

Optics EXPRESS

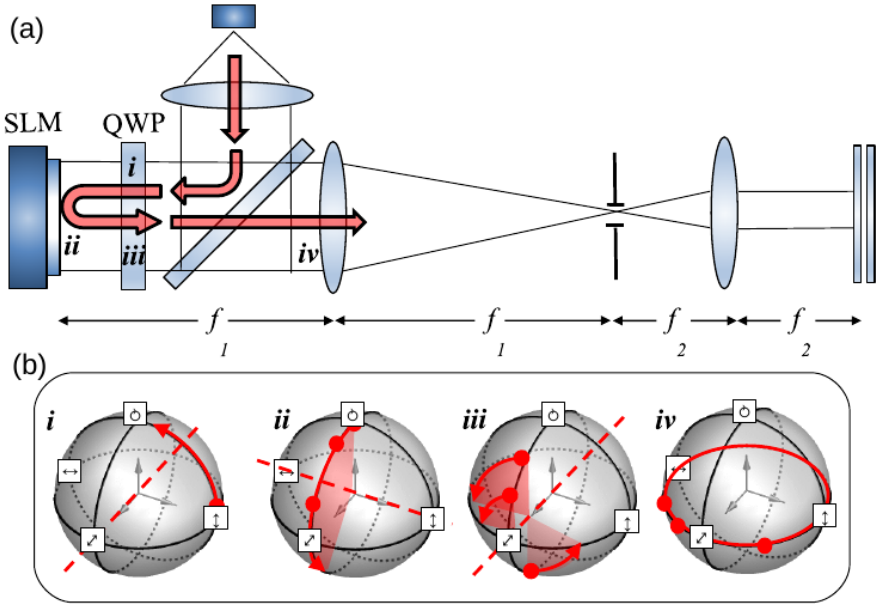

Fig. 2. (a) Optical train for polarization modulation, along with (b) the Poincare sphere representation of its operation. (i) The initially s-polarized beam makes its first pass through the quarter-wave plate (QWP) with optic axis oriented at 45deg, and becomes circularly polarized. (ii) The beam is reflected from the LCoS spatial light modulator (SLM), each pixel of which acts as an independently variable waveplate. The accessible polarization states trace out an arc on the Poincare sphere. (iii) A second pass through the QWP maps each of these polarization states back to a different linear polarization state. (iv) Crucially, as long as the retardance of the SLM pixels can be modulated through a full 2π of phase, all linear polarizations are accessible. Finally, the SLM plane is imaged onto the photoalignment cell, with a Fourier plane filter to reject higher diffracted orders.

In short, this approach allows independent and fully arbitrary control of the linear polarization angle imparted to each pixel, enabling high-throughput recording of the entire active area of the alignment cell (order 1 cm x 1 cm) at display resolution in a single exposure of 15 seconds. To validate this technique, we pattern the cubic phase profile which, following Ref. [19], is known to generate the 2D Airy beam in the Fourier plane. Solely for the purpose of visualizing the recorded alignment pattern, we introduce a thin layer of nematic liquid crystal (Fig. 3).

First, alignment cells are constructed according to previously reported procedures [36]. Photoalignment dye (PAAD-22, BEAM Co) is spin-coated onto indium-tin-oxide (ITO) coated glass slides. A pair of slides are glued together using optical adhesive mixed with glass spacer beads to ensure a uniform cell thickness of 30 μm. The patterned photoalignment exposure is 160 mW/cm^2 as measured at the sample for 15 seconds, using a 445 nm DPSS laser. The cell is then capillary filled with a previously reported formulation used to prepare PSCLCs, comprised of 0.4% photoinitiator (Irgacure 369, BASF), 6% chiral liquid crystal monomer (CMO4151, AlphaMicron, Inc), two right handed chiral dopants (6% R1011 and 5% R811, Merck), and 82.6wt% nematic liquid crystal with negative dielectric anisotropy (ZLI-2079, Merck) [36]. Upon filling, the liquid crystal orientation conforms to the patterned initial helix angle landscape (patterned on both sides). Subsequent room-temperature exposure to UV light (100mW/cm^2 for 5 min) induces photopolymerization of the stabilizing polymer network, after which the element is shelf-stable.

Optics EXPRESS

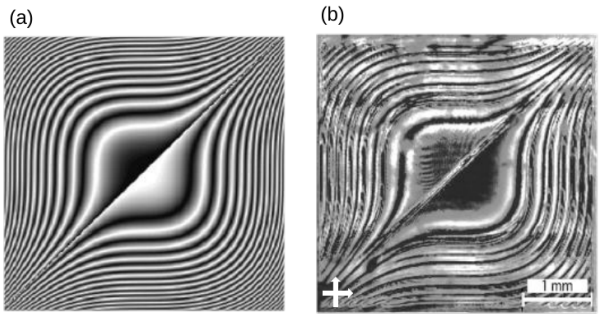

Fig. 3. 2D cubic phase mask to generate Airy beam. (a) Computer generated wrapped phase mask based on a total absolute phase change of 20π across a 4 mm x 4 mm area; white and black areas correspond to 0 and 2π phases respectively and therefore 0 and π initial helix angles. (b). Polarized optical micrograph to confirm the recording of the desired pattern into the alignment layer. For this figure only, a layer of nematic liquid crystal 5CB has been added for visualization.

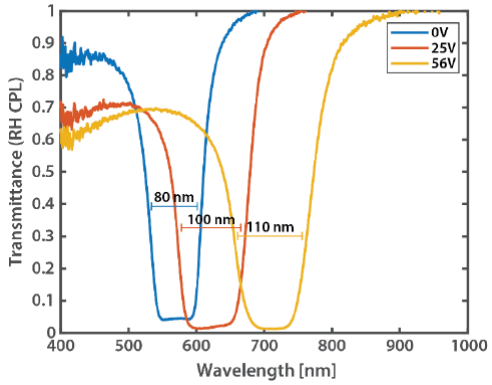

Fig. 4. Reflection band of PSCLC cell is red-shifted by applied voltage. Transmittance spectra are measured for right-circularly polarized light, matching the handedness of the PSCLC formulation. At zero applied voltage, the reflection band is centered at 570 nm with FWHM of 80 nm. When a DC voltage of 56 V is applied, the reflection band shifted to 715 nm with 110 nm FWHM.

3. Device characterization and results

We confirm via spectrometry that this PSCLC formulation exhibits a distinct reflection band, and that an applied DC voltage induces a red shift in this band, along with a slight broadening, consistent with previously reported values for this formulation (Fig. 4). We note that all recorded transmission values are normalized to account for the expected Fresnel losses at each uncoated glass/air interface. The helical half-pitch of the PSCLC is variable and can be inferred from the Bragg reflection condition converying a half-pitch ranging from 170-210 nm. We note that the tuning effect is attributed to an ion-mediated electromechanical distortion of the polymer stabilizing network [36].

Finally, we combine the pixelated phase modulation of the Bragg-reflected phase front with electrical tuning of the Bragg reflection band. As a result, when the element is illuminated with multiple beamlines (here: 532 nm and 633 nm), an Airy beam is generated in reflection at one of these colors, in a dynamically tunable way (Fig. 5). We note that the appearance of the reflected spots in the captures are attributable to Fresnel reflections or unwanted internal

Optics EXPRESS

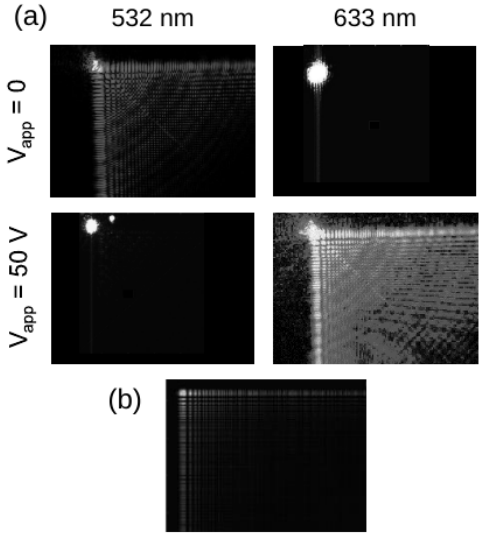

Fig. 5. (a) Far-field CCD images of reflection from element illuminated by multiple beamlines at 532 nm and 633 nm, demonstrating electrically switchable generation of Airy beams. CCD image dimensions are 6.4 x 4.8 mm. (b) Theoretical 2D Airy beam intensity distribution, for comparison.

reflections in the sample. Furthermore, these proof-of-concept diffraction elements seem to suffer a limited diffraction efficiency (about 10%) which, in principle, can be improved in the fabrication process and are not indicative of any fundamental limitation. Finally, there is an apparent quality difference between the theoretical and experimental 2D Airy patterns. We conjecture that imperfections in the SLM calibration curve (phase retardation vs voltage) lead to imperfections in the angle profile. We also note that these elements are not AR-coated, and thus unwanted internal reflections are expected to lead to either blurring or in the case of high angular bandwidth elements, “ghost" images.

To further emphasize the generality of this approach, we repeat the same experiment with other phase landscapes (Fig. 6). Firstly, we generate higher-order non-diffracting beams. As a representative example, we consider the class of Mathieu beams (corresponding to eigenmodes, in elliptical cylindrical coordinates, of Maxwell’s equations). In general, a Mathieu beam is described by the order (or charge) parameter, m, and the ellipticity parameter q, expounded upon in Refs [22, 37]. For the sake of straightforward comparison, we replicate a Mathieu beam with q = 6 and m = 27 appearing in Ref [11]. As expected, the far-field intensity profile exhibits six radial lobes, corresponding to the chosen topological charge q = 6.

Next, as a final demonstration of the versatility of this phase modulation approach, we impose a computer-generated hologram, retrieved using the standard Gerchberg-Saxton algorithm, to create a fully arbitrarily chosen intensity distribution (the text "AFRL").

In summary, we have demonstrated an optical element which selectively imposes a Pancharatnam-Berry phase upon reflection for a particular color band, where this reflection band can be dynamically shifted via an applied voltage. We emphasize that the phase modulation and the reflection band can be orthogonally designed. The unique optical re-configurability is enabled by dictating the local helical landscape on the surfaces of the PSCLC elements to produce a cubic geometric phase therefore leading to the production of a 2D Airy beam.

This technique offers a new flexible paradigm for wavefront shaping. Facile and low-

Optics EXPRESS

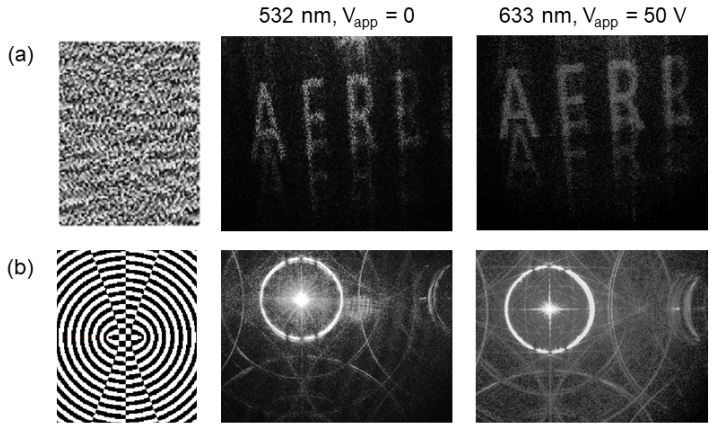

Fig. 6. Additional helix angle landscapes, and the corresponding far-field generated beams. CCD image dimensions are again 6.4 x 4.8 mm. (a) Computer-generated hologram, calculated via the Gerchberg-Saxton algorithm to spell out "AFRL". (b) Mathieu beam with q = 6, m = 27 (these parameters are related to the radial and angular portions of Mathieu functions [22, 37]). Slight defocus to show characteristic caustic curves.

cost fabrication is achieved by exploiting the self-assembly of chiral Bragg structures in PSCLCs, combined with rapid, non-contact photopatterning. This approach can straightforwardly incorporate the various electrical tuning and switching behaviors previously demonstrated in PSCLCs. Furthermore, arbitrary wavefronts can readily be encoded, enabling the generation of other exotic beam modes or other optical functionalities such as polarization-selective beam steering. Finally, this approach should also prove applicable to flexible, freestanding optical elements.

Funding

Air Force Research Laboratory and the Air Force Office of Scientific Research.

Acknowledgments

This research was performed while MSM held an NRC Research Associateship award.

Disclosures

The authors declare that there are no conflicts of interest related to this article

References

1. M. Rafayelyan, G. Tkachenko, and E. Brasselet, "Reflective spin-orbit geometric phase from chiral anisotropic optical media," Phys. Rev. Lett. **116**, 253902 (2016).
2. R. Barboza, U. Bortolozzo, M. G. Clerc, and S. Residori, "Berry phase of light under bragg reflection by chiral liquid-crystal media," Phys. Rev. Lett. **117**, 053903 (2016).
3. J. Kobashi, H. Yoshida, and M. Ozaki, "Planar optics with patterned chiral liquid crystals," Nat. Photonics **10**, 389 (2016).
4. M. Rafayelyan and E. Brasselet, "Bragg-berry mirrors: reflective broadband q-plates," Opt. Lett. **41**, 3972–3975 (2016).
5. J. Kobashi, H. Yoshida, and M. Ozaki, "Polychromatic optical vortex generation from patterned cholesteric liquid crystals," Phys. Rev. Lett. **116**, 253903 (2016).
6. M. G. Nassiri and E. Brasselet, "Pure and achromatic spin-orbit shaping of light from fresnel reflection off space-variant anisotropic media," Phys. Rev. A **99**, 013836 (2019).
7. P. Chen, L.-L. Ma, W. Duan, J. Chen, S.-J. Ge, Z.-H. Zhu, M.-J. Tang, R. Xu, W. Gao, T. Li, W. Hu, and Y.-Q. Lu, "Digitalizing self-assembled chiral superstructures for optical vortex processing," Adv. Mater. **30**, 1705865 (2018).

Optics EXPRESS

8. B.-Y. Wei, P. Chen, S.-J. Ge, W. Duan, W. Hu, and Y.-Q. Lu, "Generation of self-healing and transverse accelerating optical vortices," Appl. Phys. Lett. **109**, 121105 (2016).
9. B.-Y. Wei, S. Liu, P. Chen, S.-X. Qi, Y. Zhang, W. Hu, Y.-Q. Lu, and J.-L. Zhao, "Vortex Airy beams directly generated via liquid crystal q-Airy-plates," Appl. Phys. Lett. **112**, 121101 (2018).
10. B.-Y. Wei, P. Chen, W. Hu, W. Ji, L.-Y. Zheng, S.-J. Ge, Y. Ming, V. Chigrinov, and Y.-Q. Lu, "Polarization-controllable Airy beams generated via a photoaligned director-variant liquid crystal mask," Sci. Reports **5**, 17484 (2015).
11. S. Chávez-Cerda, M. Padgett, I. Allison, G. New, J. C. Gutiérrez-Vega, A. OâĂŹNeil, I. MacVicar, and J. Courtial, "Holographic generation and orbital angular momentum of high-order mathieu beams," J. Opt. B: Quantum Semiclassical Opt. **4**, S52 (2002).
12. H. Yoshida and J. Kobashi, "Flat optics with cholesteric and blue phase liquid crystals," Liq. Cryst. **43**, 1909–1919 (2016).
13. J. Kobashi, H. Yoshida, and M. Ozaki, "Broadband optical vortex generation from patterned cholesteric liquid crystals," Mol. Cryst. Liq. Cryst. **646**, 116–124 (2017).
14. M. Rafayelyan, G. Agez, and E. Brasselet, "Ultrabroadband gradient-pitch bragg-berry mirrors," Phys. Rev. A **96**, 043862 (2017).
15. M. G. Nassiri, S. Y. Cho, H. Yoshida, M. Ozaki, and E. Brasselet, "High-order laguerre-gauss polychromatic beams from bragg-berry flat optics," Phys. Rev. A **98**, 063834 (2018).
16. M. Rafayelyan and E. Brasselet, "Spin-to-orbital angular momentum mapping of polychromatic light," Phys. review letters **120**, 213903 (2018).
17. M. V. Berry and N. L. Balazs, "Nonspreading wave packets," Am. J. Phys. **47**, 264–267 (1979).
18. G. A. Siviloglou and D. N. Christodoulides, "Accelerating finite energy Airy beams," Opt. Lett. **32**, 979–981 (2007).
19. G. Siviloglou, J. Broky, A. Dogariu, and D. Christodoulides, "Observation of accelerating Airy beams," Phys. Rev. Lett. **99**, 213901 (2007).
20. M. A. Bandres, I. Kaminer, M. Mills, B. Rodríguez-Lara, E. Greenfield, M. Segev, and D. N. Christodoulides, "Accelerating optical beams," Opt. Photonics News **24**, 30–37 (2013).
21. M. A. Bandres, J. C. Gutiérrez-Vega, and S. Chávez-Cerda, "Parabolic nondiffracting optical wave fields," Opt. Lett. **29**, 44–46 (2004).
22. J. C. Gutiérrez-Vega, M. Iturbe-Castillo, and S. Chávez-Cerda, "Alternative formulation for invariant optical fields: Mathieu beams," Opt. Lett. **25**, 1493–1495 (2000).
23. I. Kaminer, R. Bekenstein, J. Nemirovsky, and M. Segev, "Nondiffracting accelerating wave packets of maxwellâĂŹs equations," Phys. Rev. Lett. **108**, 163901 (2012).
24. P. Zhang, Y. Hu, T. Li, D. Cannan, X. Yin, R. Morandotti, Z. Chen, and X. Zhang, "Nonparaxial mathieu and weber accelerating beams," Phys. Rev. Lett. **109**, 193901 (2012).
25. N. K. Efremidis and D. N. Christodoulides, "Abruptly autofocusing waves," Opt. Lett. **35**, 4045–4047 (2010).
26. D. G. Papazoglou, N. K. Efremidis, D. N. Christodoulides, and S. Tzortzakis, "Observation of abruptly autofocusing waves," Opt. Lett. **36**, 1842–1844 (2011).
27. P. Polynkin, M. Kolesik, J. V. Moloney, G. A. Siviloglou, and D. N. Christodoulides, "Curved plasma channel generation using ultraintense Airy beams," Science **324**, 229–232 (2009).
28. W. Nelson, J. Palastro, C. Davis, and P. Sprangle, "Propagation of bessel and Airy beams through atmospheric turbulence," J. Opt. Soc. Am. A **31**, 603–609 (2014).
29. J. Nylk, K. McCluskey, S. Aggarwal, J. A. Tello, and K. Dholakia, "Enhancement of image quality and imaging depth with Airy light-sheet microscopy in cleared and non-cleared neural tissue," Biomed. Opt. Express **7**, 4021–4033 (2016).
30. T. Vettenburg, H. I. Dalgarno, J. Nylk, C. Coll-Lladó, D. E. Ferrier, T. Čižmár, F. J. Gunn-Moore, and K. Dholakia, "Light-sheet microscopy using an Airy beam," Nat. Methods **11**, 541 (2014).
31. Z. Zheng, B.-F. Zhang, H. Chen, J. Ding, and H.-T. Wang, "Optical trapping with focused Airy beams," Appl. Opt. **50**, 43–49 (2011).
32. Y. Li, Y. Liu, S. Li, P. Zhou, T. Zhan, Q. Chen, Y. Su, and S.-T. Wu, "Single-exposure fabrication of tunable pancharatnam-berry devices using a dye-doped liquid crystal," Opt. Express **27**, 9054–9060 (2019).
33. H. Dai, X. Sun, D. Luo, and Y. Liu, "Airy beams generated by a binary phase element made of polymer-dispersed liquid crystals," Opt. Express **17**, 19365–19370 (2009).
34. D. Luo, H. Dai, and X. Sun, "Polarization-independent electrically tunable/switchable Airy beam based on polymer-stabilized blue phase liquid crystal," Opt. Express **21**, 31318–31323 (2013).
35. I. Moreno, J. A. Davis, T. M. Hernandez, D. M. Cottrell, and D. Sand, "Complete polarization control of light from a liquid crystal spatial light modulator," Opt. Express **20**, 364–376 (2012).
36. K. M. Lee, V. P. Tondiglia, T. Lee, I. I. Smalyukh, and T. J. White, "Large range electrically-induced reflection notch tuning in polymer stabilized cholesteric liquid crystals," J. Mater. Chem. C **3**, 8788–8793 (2015).
37. R. Hernández-Hernández, R. Terborg, I. Ricardez-Vargas, and K. Volke-Sepúlveda, "Experimental generation of mathieu–gauss beams with a phase-only spatial light modulator," Appl. Opt. **49**, 6903–6909 (2010).